Flexible Dielectric Nanocomposites with Ultra-Wide Zero Temperature Coefficient Window for Electrical Energy Storage and Conversion under Extreme Conditions

Khurram Shehzad[‡], Yang Xu[‡‡,*], Chao Gao[§], Hanying Li[§], Zhi-Min Dang[‖], Tawfique Hasan[⊥], Jack Luo[‡▽], and Xiangfeng Duan[‡*]

[‡]College of Information Science and Electronic Engineering, Zhejiang University, Hangzhou 310027, China

[‡]Department of Chemistry and Biochemistry and California Nanosystems Institute, University of California, Los Angeles, California 90095, United States

[§]MOE Key Laboratory of Macromolecular Synthesis and Functionalization, Zhejiang University, Hangzhou 310027, China

[‖]State Key Laboratory of Power System, Department of Electrical Engineering, Tsinghua University, Beijing 100084, China

[⊥] Cambridge Graphene Centre, University of Cambridge, Cambridge, CB3 0FA, UK

[▽]Institute for Materials Research and Innovation, The University of Bolton Deane Road, Bolton, BL3 5AB, UK

[*]E.mail: yangxu-isee@zju.edu.cn, xduan@chem.ucla.edu

ABSTRACT

Polymer dielectrics offer key advantages over their ceramic counterparts such as flexibility, scalability, low-cost, and high-breakdown voltages. However, a major drawback that limits more widespread application of polymer dielectrics is their temperature-dependent dielectric properties. To achieve dielectric constants with low/zero temperature coefficient (L/0TC) over a broad temperature range is essential for applications in diverse technologies. Here, we report a hybrid filler strategy to produce polymer composites with an ultra-wide L/0TC window of dielectric constant, as well as significantly enhanced dielectric value, maximum energy storage density, thermal conductivity and stability. By creating a series of percolative polymer composites, we demonstrated hybrid carbon filler based composites can exhibit zero-temperature coefficient window of 200 °C (from −50°C to 150°C), a widest 0TC

window for all polymer composite dielectrics reported to date. We further show the temperature coefficient of the composites is highly stable against stretching and bending, even under AC electric field with frequency up to 1 MHz. We envision that our method will push the functional limits of polymer dielectrics for flexible electronics in extreme conditions such as in hybrid vehicles, aerospace, power electronics, and underground oil/gas exploration.

Keywords: Dielectric constant; Polymer nanocomposites; Zero temperature coefficient; Carbon nanotubes; Energy storage and conversion

INTRODUCTION

Dielectrics can deliver a very high power density and represent an attractive rapid energy storage technology for applications in hybrid vehicles, power electronics, bio-medical field, and electrical weapon systems.[1-3] Compared to the ceramic dielectrics, polymer dielectrics offer a high breakdown voltage, lower processing temperature, easy processibility, flexibility, and are of increasing interest for diverse applications.[4] However, polymers typically have intrinsically low dielectric constants (e.g., < 10). It is thus often necessary to form composites of polymers with dielectric or conductive fillers to raise their dielectric constant for variety of high energy density applications. Percolative polymer composites (PPCs), containing a conductive filler, achieve high dielectric constant at relatively low filler concentrations while retaining the easy processibility and mechanical robustness of polymer composites, making them a key multi-functional material for applications in energy conversion and storage,[5-6] electronics,[7] and bio-medical fields.[8-9] Despite their widespread applications and advantageous properties, PPCs are typically limited by intrinsic drawbacks of sharp insulator-conductor transition near the percolation threshold, and highly temperature dependent electric and dielectric properties.[10-11] Compared to the electrical resistivity (ρ), the dielectric constant (κ) of PPCs is much more sensitive to the temperature since the filler concentration of composites with high dielectric constant and low dielectric loss always falls

in the most thermal-sensitive region of percolation curve (near the critical filler concentration).[10, 12] This intrinsic drawback limits the working temperature of PPCs, and makes them unsuitable for the applications with large temperature swings such as in hybrid vehicles, aerospace, power electronics, and underground oil/gas exploration.[13-15] In fact, temperature sensitivity of κ is a challenge not only for PPCs, but also for traditional ceramic capacitors used in electronic circuits. To achieve the stable function of ceramic capacitors over a wide temperature window, complex temperature compensating electronic circuits are required.

To enhance the applicability of PPCs, low/zero temperature coefficients of dielectric constant (L/0TC$_\kappa$), as well as electrical resistivity (L/0TC$_\rho$), over a broad temperature range is much needed. So far there is no comprehensive strategy available to simultaneously obtain both the wide temperature range L/0TC$_\kappa$ and L/0TC$_\rho$ in PPCs. Strategies such as polymer-filler interface engineering[16-18] or filler alignment[19-20] have been employed for this purpose. However, despite considerable efforts with different strategies, L/0TC was achieved only over a relatively narrow temperature window (e.g., 100 °C). A most recent breakthrough reports nanocomposites with relatively high working temperature[21], yet with relatively low dielectric constant (~3.5 at maximum), and thus unsuitable for high energy density storage materials.

Herein, we report a novel hybrid filler strategy for tailoring the temperature dependence of dielectric as well as the electrical resitivity of the PPCs. By using hybrid of one–dimensional (1D) carbon nanotubes (CNTs) and common zero–dimensional (0D) carbon black (CB)fillers, we simultaneously achieved L/0TC$_\kappa$ and L/0TC$_\rho$ in the hybrid filler composites over a record ultra-wide temperature window of 200°C (from −50 °C to 150 °C), which is at least 2 times wider than those of single filler based polymer composites reported previously. Moreover, L/0TC properties are highly stable against stretching and bending, even under AC electric field with frequency up to 1 MHz. By controlling the concentration and

relative ratio of hybrid constituent fillers, we demonstrate, for the first time, that PPCs can be engineered to achieve positive, negative and zero temperature coefficients of resistance (PTC_ρ, NTC_ρ, $L/0TC_\rho$) by design, which can open up many exciting opportunities for practical applications such as temperature sensing and self-regulating heating.

RESULTS AND DISSCUSION

Polymer composites were fabricated by melt mixing the polymers, and the individual (CNT, and CB) as well as their hybrid fillers (CNT-CB). Initially two types of CNTs were studied, but finally one type was chosen due to its better suitability for our studies (details of the process and choice of materials for fabrication of polymer composites are provided in the supporting information). By controlling the relative ratio of hybrid fillers in the composites, it is possible to achieve L/0TC PPC over a wide temperature window. Figure 1a shows the TEM images of CNT, CB, and (CNT+CB) hybrid fillers, while the Fig. 1c describes the schematics of filler networks in the thermoplastic elastomer (TPE) polymer matrix. For CNT+CB hybrid filler, CB particles or clusters are bridged by CNTs as shown by TEM image. Cross sectional SEM images (Fig. 1b) confirm the presence of CNT, CB, and CNT+CB fillers in their respective composites. Figure 2 shows the dependences of of κ and ρ on the volume fraction of different carbon fillers at room temperature. Figure 2 clearly demonstrated a conductor-insulator translation in the volume fraction range of 0.06-0.07, for all carbon fillers. A large enhancement in the electrical conductivity (σ) of several orders of magnitude was observed at critical concentration (percolation threshold), indicating the formation of the continuous conductive network in the nanocomposites. A large enhancement in dielectric permittivity (ε) of nanocomposites was also observed near (below) this critical concentration, which was the result of Maxwell-Wagner-Sillar polarization. Electrical resistivity and dielectric constant of the typical PPCs are generally governed by the following formula: [22-24]

$$\rho \propto (f_{\text{filler}} - f_{\text{c}})^{t}, \quad \text{for} \quad f_{\text{c}} \leq f_{\text{filler}} \tag{1}$$

$$\kappa \propto (f_c - f_{filler})^{-q}, \quad \text{for} \quad f_c \geq f_{filler} \tag{2}$$

where f_{filler} is the filler concentration, f_c is the percolation threshold, and q and t are the critical constants. Linear fitting of Eq. 1 and 2 produced the percolation threshold as 0.06, 0.07, and 0.07, values of q as 0.87, 1.44, and 0.57, and values of t as 1.06, 4.50, and 4.63, for CNT, CB, and (CNT+CB) based composites, respectively (Fig. S1). For 3D fillers, universal value of t is in the range of 1.6–2.0 while of q is 1.0. Non-universal and high value of t can be attributed to diverging inter-particle distances (caused by variations in aspect ratios, dispersion and the networks of filler in the polymer matrix), yielding a diverging distribution of resistance elements as inter-particle resistance bare the feature of exponential decay of tunneling conductivity with the inter-particle distance. [23, 25] A lower t value also means a more sharper percoaltion curve, and higher t value corresponds to a more gradual percoaltion curve. Dielectric loss tangent of the all the polymer composites is provided in Fig. S2a. Dependence of dielectric constant and dielectric loss tangent against the AC frequencies at selected concentration (0.06) of hybrid filler is also provided in Fig. S2b. Percolation threshold of our CNT/polymer composites is relatively high but still consistent with previous studies.[26-27] A higher than expected peroclation threshold of CNTs is probably result of waviness/flexibility of CNTs which make them bend and consequently lower their effective length and/or aspect ratio. Percolation threshold of hybrid fillers was in close approximation of previously proposed theoretical models which propose the equation $V_{CNT}/f_{CNT} + V_{CB}/f_{CB} = 1$ to calculate the percolation threshold for mixed fillers.[23]

Figure 3a and 3b present the effect of temperature on κ and ρ of all the composites, respectively. For comaprison, temeprature dependence of pure polymer matrices (TPE and PVDF) is also presented in Supplementary Fig. S3. There is no obvious correlation temeprature dependence of dielectric properties between of pure polymers and their composites, as properties of pure polymer at various temperatures are determined by chain

dynamics, while of composites are determinded by filler networks. TPE composites with 0D filler (CB) exhibit obvious temperature dependent electrical and dielectric properties, especially near melting temperature of TPE (150 °C) (Fig. S3), where κ decreases and ρ increases (PTC effect) with increasing temperature (To be consistent with literature and to avoid confusion, the term L/0TC will be used for both ρ and κ, and the terms PTC and NTC in following discussion will be only used with reference to electrical resistivity but not to dielectric constant). Variety of mechanisms (such as volume exapnsion, tunneling current migration of filler particles, electric field emission, and internal stress) have been reported in the literature to explain the PTC effect. Most probable mechanism in thise case may be the thermal expansion of polymer, which took place at the melting point of the polymer matrix, resulted in the break-up of the conducting chains (see schematics in Fig. S4), with a consequent increase in ρ and decrease in κ value of the composites. [28-30] It is important to note that due to the 0D nature of CB particles, contact between CB particles is point-type, whcih is easily breakable.

In the case of 1D (CNT) filler based polymer composites, compared to CB where inter-filler point-type contact has low contact area, inter-CNT line-type contact, due to the large aspect ratio (AR) of CNTs because fo their 1D nature, has larger contact area (the schematics of NTC mechanism for CNT based composites is presented in Fig. S4). It is important to mention that some of the CNTs, when not oriented parallele to each other, may also have point-type contact. However, point-type contact of CNTs is not easy to break becase of thier higher length. These factors make CNT/polymer composites immune to polymer chain movement induced increase in ρ. Instead, just below the percolation threshold, CNT/polymer composites show a decrease in ρ and an increase in κ values at higher temperatures (Fig. 3a, 3b). For example, near percolation threshold, the κ value of the composites experiences an increase of at least 75% in the temperature range of −50 °C to 150 °C. The decrease in

resistivity and increase in κ with temperature is often ascribed to temperature dependent increase in the conductivity of polymer matrix, thermal fluctuations induced tunneling (FIT),[31-32] variable range hopping (VRH),[33] or reparation of the disconnected conductive chains due to the dynamic factors (van der Waals interaction between fillers).[34-35]

Since CNT and CB based composites display opposite temperature dependence of their electrical and dielectric properties, we hypothesize that a combination of both fillers in appropriate ratio could result in a balance to create a composite with temperature independent electrical/dielectric properties. Indeed, by adding an equal concentration of CB and CNT [$(CNT_{(0.03)} + CB_{(0.03)})$, where 0.03 in subscript means the volume fraction of each filler], we obtain a balanced composite where CB induced fall in κ is compensated by a CNT induced increase in κ (Fig. 4a). The figure presents the normalized electrical resistivity [$\rho(T)/\rho_{-50°C}$], and the percentage change in κ against its value at −50 °C. $\rho(T)$ is resistivity at a given temperature and $\rho_{-50°C}$ is resistivity at −50 °C. Normalized resistivity values and change in κ, with reference to their room temperature value are also presented in Figs. S6-S8.

Figure 4c shows that ρ and κ values display no significant change over the entire investigated temperature range of −50 to 150 °C, clearly demonstrating that an unprecedented wide $L/0TC_\rho$ and $L/0TC_\kappa$ window has been achieved in (CNT+CB)/polymer composites with 0.06 filler volume fraction. In contrast to a maximum change of 125% in k for CNT composite and −42% for CB composite over the temperature range of −50 to 150 °C, the maximum change in k of CNT+CB hybrid composite is only 9.7% (Fig. S5b). By using the room temperature (25 °C) as reference, the maximum change of k in the temperature range of −50 to 150 °C is also only 9.2% (Fig. S6b). Similarly, temperature coefficient of dielectric constant (τ_κ) for hybrid filler is 59 parts per million (p.p.m.) per °C compared to −640 p.p.m. per °C for CB and 2447 p.p.m. for CNT based composites, respectively, within the temperature range of −50 to 150 °C (Fig. 5). Because the operating temperature range for

most of the electronic devices falls in −55 to 150 °C, the weak-temperature dependence of κ in this temperature range is extremely important. Variation of the κ against temperature for our L/0TC$_\kappa$ composites fully satisfies the X8P EIA (Electronic Industries Association) specification[36] which requires the variation of the capacitance in the temperature interval from −55 to 150 ^{o}C to be less than ± 10% of its room temperature (25 ^{o}C) value for a capacitor. Importantly, in this temperature window, percent changes in dielectric loss tangent of our hybrid filler composite were quantitatively on the same level as dielectric constant (<~10 %) and hence also exhibited the L/0TC characteristics (Fig. S9).

Since our polymer matrix is an elastomer, it is interesting to investigate the effects of physical bending and stretching on the L/0TC$_\sigma$ and L/0TC$_\kappa$ characteristics. Multiple bending cycles didnt show any significant change in the mechanical properties of composites, indicating their good service life (Table S2). Figure 6a shows that composites retain their L/0TC$_\rho$ and L/0TC$_\kappa$ even after 3000 cyclic bending. Compared to bending, where strain is relatively small (usually below 1%)[37], it is more challenging to retain the L/0TC properties for stretchable devices where the strain is much larger. We stretched the composite samples up to 15% and found that the composites retain their L/0TC characteristics, as shown in Fig. 6b. These results demonstrated that our L/0TC composites have excellent properties and could be very useful for flexible electronics. We further tested the L/0TC$_\sigma$ and L/0TC$_\kappa$ properties at different AC frequencies (100 Hz, 10 kHz and 1 MHz). As evident in Fig. 6c, at lower frequencies and high temperature (>120 ^{o}C), L/0TC$_\kappa$ characteristics are relatively poor. With increasing frequency, L/0TC$_\kappa$ improves, probably because of fall in initial κ values of the composites. The decrease in the κ values of PPCs with frequencies, especially below 10^4 Hz, is a common phenomenon associated with relaxation in inter−phase polarization[22] between the conductive filler and the insulating polymer matrix. The changes in the L/0TC$_\rho$ (red lines in Fig. 6c) with frequency may also arise from the frequency dependent variation in ρ, as below

the percolation threshold, ρ presents a critical behavior against the AC frequencies.[22] Apart from the L/0TC$_\rho$ and L/0TC$_\kappa$, our hybrid filler polymer composites, compared to the neat polymer also show significant enhancement of dielectric constant by 50 times (Fig. 1d), reasonable dielectric breakdown strength (Fig. S10), thermal conductivity by over 100% (increased from ~ 0.12 W m^{-1} K^{-1} for pure polymer to ~ 0.30 W m^{-1} K^{-1} for 0.06 volume fraction hybrid filler composites), and thermal stability by 29% (Fig. S3b).

To test the versatility of our concept for other polymer matrix, we have also fabricated (CNT+CB) hybrid filler PPCs using dielectric polymer polyvinylidene fluoride (PVDF). By adjusting the ratio of CNT and CB in hybrid filler, L/0TC$_\rho$ and L/0TC$_\kappa$ characteristics of PVDF based composites are obtained at a filler combination of CNT $_{(0.030)}$ + CB $_{(0.035)}$. Compared to TPE based composites, the PVDF based composites display even better L/0TC$_\kappa$ properties (Fig. 6d), especially at higher temperatures. The variation in κ was less than ± 10% at 150 ^{o}C, thus fully satisfying the X8P EIA specification.[36] Note that contrary to TPE composites, where L/0TC characteristics are obtained at equal filler concentrations of CNT and CB (e.g. 0.03 volume fraction for each filler), L/0TC$_\rho$ and L/0TC$_\kappa$ characteristics for (CNT+CB)/PVDF composites were obtained at different filler volume fractions of each filler (0.03, and 0.035 volume fraction of CNT and CB, respectively). Results from PVDF composites indicate that our strategy could be potentially applied to other polymers. Maximum energy density (U_{max}) of both the TPE and PVDF based composites calculated by expression $U_{max} = \kappa\varepsilon_0 E_b^2/2$, where κ is the dielectric constant of the composites, E_b is the electric breakdown field, ε_0 is the vacuum dielectric permittivity (8.85×10^{-12} F/m),[3] was in the range of 0.05−3.2 J/cm^3, close to state−of−the art dielectric polymer BOPP (3.5−4 J/cm^3).[3] At 0TC concentration, the U_{max} for both the TPE and PVDF based composites was 0.17, and 2.80 J/cm^3, respectively. Main advantage of our composite is resonably high energy density without any significant change over a wide temeprature window. Energy density of

dielectric composites can be further improved by choosing polymer matrix with better breakdown strength and by using the modified core-shell filler structures, however, main focus of this work is to demonstrate the temeprature independent properties of dielectric composites over an ultra-wide temperature range. Breakdown strength and maximum energy density of both TPE and PVDF based composites at different hybrid filler concentrations are given in Fig. S10.

For high-κ materials, only L/0TC property is sought and other modes of temperature dependence are not required. While for conductors, all mode of variation in electrical resistivity with temperature (PTC$_\rho$, NTC$_\rho$, L/0TC$_\rho$) are useful for practical applications.[38] We find that by changing the relative concentration or/and total concentration of fillers we can engineer the same composites system for any temperature coefficient of electrical resistivity with desired level of ρ and intensity of respective temperature coefficient. Furthermore, it is also possible to tune the initial ρ and κ value of the composites without changing the mode of temperature coefficient (see supporting section S1). We believe that value of temperature coefficient of a single filler based composite at specific filler concentration, rather simply the concentration of filler, may be much more rational parameter while deciding the composition of a hybrid filler composite to achieve the certain mode of temperature coefficient. This is the reason why in the case of PVDF based composites, different concentrations of CB and CNT rather the equal concentration achieved the L/0TC properties. Value of the temperature coefficient of a single filler based composite will depend upon the polymer matrix, and the percolation characteristics such as shape of the percolation curve, percolation threshold and value of the critical constants (supporting section S1).

Figure 7a compares our results with previous literatures on different dielectric materials including ceramics[39-40], ceramic based composites[41-42] and PPCs[10, 43 17, 19-20] and shows widest L/0TC$_\kappa$ window for our composites that is nearly two times wider than previously achieved

value. Also compared to earlier reports on the percolative dielectric polymer composites based on particle[17, 43] or rod-like fillers,[26-27] our hybrid filler approach offers a much wider (almost 2 times) L/0TC window of 200 ^{o}C (−50 to 150 ^{o}C). Usually, temperature induced variations in electrical or dielectric properties of PPCs are results of thermal transitions in polymers. Our hybrid filler strategy together with polymer matrix which has suppressed thermal transitions, such as recently reported low-*k* cross-linked polymer nanocomposites with boron nitride nanosheets fillers,[21] can allow even further extension of L/0TC$_{\kappa}$ and L/0TC$_{\rho}$ windows. Such an outcome can possibly lead to applicability of PPCs at even further higher temperatures compared to what we reported here.

We believe that this hybrid filler strategy is not limited only to CNT and CB but could also be extended to other conducting fillers of different shapes (plate, rod, and spheres), dimensions (1D, 2D, or 3D) and chemical nature (organic or inorganic). In particular, considering the recent surge of interest in 2D materials (graphene like)[44-46] and their composites [47-50] and the fact that these composites experience the same sort of temperature dependence as other PPCs[51-52], our hybrid filler strategy can also be helpful to grant a better control over the temperature dependence of electrical properties of such composites. This srtategy can also possibly be applied to layered composites.[53-56] Generally, composites based on particle fillers observe PTC effect due to the fact that inter-particle contact is point-type which has characteristics of low contact area.[57] On the other hand, composites based on large contact area type fillers such as with line contacts (for high aspect ratio rod like fillers)[58] or face contacts (for plate like fillers)[59] are expected to have the NTC effect (a summary of inter-filler contacts and associated temperature coefficient is provided in Fig. 7b). Therefore, careful choice of relative filler concentration of low and large contact area fillers in the hybrid can open a new rational and universal route to control the temperature dependence of electrical properties of the hybrid filler based composites.

CONCLUSIONS

We have demonstrated a hybrid filler strategy that gives extraordinary control and versatility to the design of dielectric polymer composites. Our approach allows to fabricate the polymer composites with L/0TC characteristic which is independent of physical deformation and AC frequency. Moreover, this strategy is applicable to various fillers and polymers. By changing the total concentration of CNT+CB fillers and by carefully choosing the relative ratio of CNT and CB, we can obtain all three modes of temperature dependence of ρ and κ in a single polymer composite system. Such a simple strategy grants extraordinary control and versatility in designing PPCs with controlled temperature dependence of electric and dielectric properties.

EXPERIMENTAL DETAILS

Multi-walled carbon nanotubes (CNTs) were synthesized by chemical vapor deposition method using ferrocene as catalyst precursor and toluene as a carbon source[60]. Amongst two types, CNTs with diameter, length, and specific surface area of 10 – 30 nm, 5 – 15 μm, and 90– 140 m^2/g, respectively, were chosen (see Fig. S11). 99.9 % pure Acetylene CB powder (Product No: 39724), and Polyvinylidene fluoride (PVDF) (Product No: 44080) were purchased from Alfa Aesar company. The average size of the CB particles, surface area, and bulk density was 40 nm, 75 m^2/g, and 80 – 120 g/*l*, respectively (supplier data). Dynamically vulcanized polypropylene based thermoplastic elastomer (TPE) matrix [polypropylene and copolymer of ethylene–propylene–diene monomer (PP/EPDM)] in bead form, supplied by Dawn-BH elastomer Co., Ltd., was chosen as polymer matrix.

For composite preparation, three carbon based fillers [CB, CNT and (CNT+CB) hybrid filler] were used. They were mixed with the TPE and PVDF matrix separately in a twin screw HAAKE Polydrive mixer at 180 °C for 20 min. Processing temperature was set at 180 °C, higher than melting temperature of the polymer matrix for better processing. The mixing

speed was 100 rpm. The composites were hot pressed and cut into sheets with a diameter of 12 mm and a thickness of 1 mm, at 20 MPa pressure and 200 °C temperature for 15 min. For electrical measurements, samples were pasted with silver electrodes on both sides to minimize the contact resistance. For planar capacitor structures, interdigitated Cr (15nm)/Au (50nm) electrodes were deposited on polymer sheets by using e-beam evaporation (see Fig. S12). Typical dimensions of the interdigitated electrodes were 300μm electrode width 300 μm electrode separations, 1cm electrode length. Dielectric constant of the samples was measured using an HP 4294 A impedance analyzer in the frequency range of 1 kHz to 40 MHz and temperature range of −50 to 150 ºC. Temperature scan rate was 5 °C min^{-1} with soak time of 2 min for each measurement step. The dielectric breakdown strength was measured based on IEC60243-1 standard. Ten samples for each composition were tested and the results were analyzed using Weibull statistical analysis. The DC volume resistance of the samples along the thickness direction was measured by employing a digital multimeter (below 2×10^7 Ω) and a ZC-36 megger (above 2×10^7 Ω) at progressively elevated temperatures. Rate of change in temperature was set as 5 °C min^{-1}. Morphology of the fillers and microstructures of the fractured surface of the composites was characterized using transmission electron microscopy (TEM, Hitachi H-800) and scanning electron microscope (SEM, Hitachi S-4700), respectively. The melting behaviors of the composites were measured by differential scanning calorimetry (DSC, DuPont TA 2910) from 25 °C to 200 °C at heating rate of 5 °C min^{-1} under N_2. Thermal stability was determined with a Perkin–Elmer TGA-7 thermo gravimetric analyzer over a temperature range of 20–700 °C at a heating rate of 5 °C/min. The thermal conductivity measurements were conducted on a Transient Hot Disk TPS 2500S instrument (Hot Disk AB, Gothenburg, Sweden) according to ISO 22007-2 standard. Mechanical properties were measured with a universal testing machine (Instron 4465) at room temperature and stretching rate of 200mm/min.

Temperature coefficient of dielectric constant

The temperature coefficient of dielectric constant (τ_κ), for a given temperature range (from T_i to T_f), is defined as:

$$\tau_\kappa = (k_f - k_i) / [\, k_{ref}(T_f - T_i)] \quad (3)$$

where k_{ref} is the dielectric constant at room temperature, T_i and T_f are the low-end and high-end temperatures, respectively, and k_i and k_f are the dielectric constants at T_i and T_f, respectively.

SUPPORTING INFORMATION. Text on all mode temperature dependence of electrical resistivity, text on the percolation characteristics of CNT/TPE composites with various aspect ratio CNTs, fitting of percolation curves, thermal transition of pure polymers and composites, schematics of temperature dependence of filler networks in polymer matrix, temperature dependent dielectric and electric properties of composites based on various combinations of hybrid fillers, dielectric loss tangent vs temperature curves, energy storage capacity of polymer composites, schematics and real images of inter-digitated electrodes, data on mechanical properties and temperature coefficients of polymer composites.

ACKNOWLEDGEMENTS

The authors would like to thank Prof. S Iijima, A. Martinez, Prof. J. Xie, and Prof. Z.M Dang for helpful discussion and comments. This work is supported by National Science Foundation of China (Grant Nos. 61006077, 61274123, 61425201, and 61474099), ZJ-NSF (LR12F04001). Y. Xu is supported by ZJU Cyber Scholarship and Cyrus Tang Center for Sensor Materials and Applications, and Visiting-by-Fellowship of Churchill College, University of Cambridge. T. Hasan is supported by The Royal Academy of Engineering (Graphlex).

References

1. Dang, Z.-M.; Zheng, M.-S.; Zha, J.-W., 1d/2d Carbon Nanomaterial-Polymer Dielectric Composites with High Permittivity for Power Energy Storage Applications. *Small* **2016,** *12* (13), 1688-1701.
2. Chen, Q.; Shen, Y.; Zhang, S.; Zhang, Q. M., Polymer-Based Dielectrics with High Energy Storage Density. *Annu. Rev. Mater. Res.* **2015,** *45*, 433-458.
3. Prateek; Thakur, V. K.; Gupta, R. K., Recent Progress on Ferroelectric Polymer-Based Nanocomposites for High Energy Density Capacitors: Synthesis, Dielectric Properties, and Future Aspects. *Chem. Rev. (Washington, DC, U. S.)* **2016,** *116* (7), 4260-4317.
4. Mannodi-Kanakkithodi, A.; Treich, G. M.; Tran Doan, H.; Ma, R.; Tefferi, M.; Cao, Y.; Sotzing, G. A.; Ramprasad, R., Rational Co-Design of Polymer Dielectrics for Energy Storage. *Adv. Mater. (Weinheim, Ger.)* **2016,** *28* (30), 6277-6291.
5. Wang, G.; Huang, X.; Jiang, P., Tailoring Dielectric Properties and Energy Density of Ferroelectric Polymer Nanocomposites by High-K Nanowires. *ACS Appl. Mater. Interfaces* **2015,** *7* (32), 18017-18027.
6. Dang, Z.-M.; Yuan, J.-K.; Yao, S.-H.; Liao, R.-J., Flexible Nanodielectric Materials with High Permittivity for Power Energy Storage. *Adv. Mater. (Weinheim, Ger.)* **2013,** *25* (44), 6334-6365.
7. Ko, J.; Kim, Y.-J.; Kim, Y. S., Self-Healing Polymer Dielectric for a High Capacitance Gate Insulator. *ACS Appl. Mater. Interfaces* **2016,** *8* (36), 23854-23861.
8. Zeng, Z.; Jin, H.; Zhang, L.; Zhang, H.; Chen, Z.; Gao, F.; Zhang, Z., Low-Voltage and High-Performance Electrothermal Actuator Based on Multi-Walled Carbon Nanotube/Polymer Composites. *Carbon* **2015,** *84*, 327-334.
9. Song, S.; Zhai, Y.; Zhang, Y., Bioinspired Graphene Oxide/Polymer Nanocomposite Paper with High Strength, Toughness, and Dielectric Constant. *ACS Appl. Mater. Interfaces* **2016,** *8* (45), 31264-31272.
10. Xu, H.-P.; Dang, Z.-M.; Bing, N.-C.; Wu, Y.-H.; Yang, D.-D., Temperature Dependence of Electric and Dielectric Behaviors of Ni/Polyvinylidene Fluoride Composites. *J. Appl. Phys.* **2010,** *107* (3), 034105.
11. Dai, K.; Zhang, Y.-C.; Tang, J.-H.; Ji, X.; Li, Z.-M., Anomalous Attenuation and Structural Origin of Positive Temperature Coefficient (Ptc) Effect in a Carbon Black (Cb)/Poly(Ethylene Terephthalate) (Pet)/Polyethylene (Pe) Electrically Conductive Microfibrillar Polymer Composite with a Preferential Cb Distribution. *J. Appl. Polym. Sci.* **2012,** *125* (S1), E561-E570.
12. Pecharromán, C.; Moya, J. S., Experimental Evidence of a Giant Capacitance in Insulator–Conductor Composites at the Percolation Threshold. *Adv. Mater. (Weinheim, Ger.)* **2000,** *12* (4), 294-297.
13. Johnson, R. W.; Evans, J. L.; Jacobsen, P.; Thompson, J. R.; Christopher, M., The Changing Automotive Environment: High-Temperature Electronics. *IEEE Trans. Electron. Packag. Manuf.* **2004,** *27* (3), 164-176.
14. Watson, J.; Castro, C., High-Temperature Electronics Pose Design and Reliability Challenges *Analog Dialog.* **2012,** *46* (4), 3-9.
15. Weimer, J. In *Electrical Power Technology for the More Electric Aircraft*, Digital Avionics Systems Conference, 1993. 12th DASC., AIAA/IEEE, IEEE: **1993**; pp 445-450.
16. Huang, X.; Jiang, P., Core–Shell Structured High‐K Polymer Nanocomposites for Energy Storage and Dielectric Applications. *Adv. Mater. (Weinheim, Ger.)* **2015,** *27* (3), 546-554.

17. Shen, Y.; Lin, Y.; Nan, C. W., Interfacial Effect on Dielectric Properties of Polymer Nanocomposites Filled with Core/Shell-Structured Particles. *Adv. Funct. Mater.* **2007,** *17* (14), 2405-2410.
18. Yang, C.; Lin, Y.; Nan, C., Modified Carbon Nanotube Composites with High Dielectric Constant, Low Dielectric Loss and Large Energy Density. *Carbon* **2009,** *47* (4), 1096-1101.
19. Yousefi, N.; Sun, X.; Lin, X.; Shen, X.; Jia, J.; Zhang, B.; Tang, B.; Chan, M.; Kim, J. K., Highly Aligned Graphene/Polymer Nanocomposites with Excellent Dielectric Properties for High‐Performance Electromagnetic Interference Shielding. *Adv. Mater. (Weinheim, Ger.)* **2014,** *26* (31), 5480-5487.
20. Dang, Z.-M.; Wu, J.-P.; Xu, H.-P.; Yao, S.-H.; Jiang, M.-J.; Bai, J., Dielectric Properties of Upright Carbon Fiber Filled Poly (Vinylidene Fluoride) Composite with Low Percolation Threshold and Weak Temperature Dependence. *Appl. Phys. Lett.* **2007,** *91* (7), 072912.
21. Li, Q.; Chen, L.; Gadinski, M. R.; Zhang, S.; Zhang, G.; Li, H.; Haque, A.; Chen, L.-Q.; Jackson, T.; Wang, Q., Flexible High-Temperature Dielectric Materials from Polymer Nanocomposites. *Nature* **2015,** *523* (7562), 576-579.
22. Shehzad, K.; Dang, Z.-M.; Ahmad, M. N.; Sagar, R. U. R.; Butt, S.; Farooq, M. U.; Wang, T.-B., Effects of Carbon Nanotubes Aspect Ratio on the Qualitative and Quantitative Aspects of Frequency Response of Electrical Conductivity and Dielectric Permittivity in the Carbon Nanotube/Polymer Composites. *Carbon* **2013,** *54*, 105-112.
23. Dang, Z.-M.; Shehzad, K.; Zha, J.-W.; Mujahid, A.; Hussain, T.; Nie, J.; Shi, C.-Y., Complementary Percolation Characteristics of Carbon Fillers Based Electrically Percolative Thermoplastic Elastomer Composites. *Compos. Sci. Technol.* **2011,** *72* (1), 28-35.
24. Shehzad, K.; Hussain, T.; Shah, A. T.; Mujahid, A.; Ahmad, M. N.; Sagar, R. u. R.; Anwar, T.; Nasir, S.; Ali, A., Effect of the Carbon Nanotube Size Dispersity on the Electrical Properties and Pressure Sensing of the Polymer Composites. *J. Mater. Sci.* **2016,** *51* (24), 11014-11020.
25. Dang, Z.-M.; Shehzad, K.; Zha, J.-W.; Hussain, T.; Jun, N.; Bai, J., On Refining the Relationship between Aspect Ratio and Percolation Threshold of Practical Carbon Nanotubes/Polymer Nanocomposites. *Jpn. J. Appl. Phys.* **2011,** *50* (8), 080214.
26. Dang, Z. M.; Wang, L.; Yin, Y.; Zhang, Q.; Lei, Q. Q., Giant Dielectric Permittivities in Functionalized Carbon-Nanotube/ Electroactive-Polymer Nanocomposites. *Adv. Mater. (Weinheim, Ger.)* **2007,** *19* (6), 852-857.
27. Yuan, J.-K.; Yao, S.-H.; Dang, Z.-M.; Sylvestre, A.; Genestoux, M.; Bai1, J., Giant Dielectric Permittivity Nanocomposites: Realizing True Potential of Pristine Carbon Nanotubes in Polyvinylidene Fluoride Matrix through an Enhanced Interfacial Interaction. *J. Phys. Chem. C* **2011,** *115* (13), 5515-5521.
28. Hu, N.; Fukunaga, H.; Atobe, S.; Liu, Y.; Li, J., Piezoresistive Strain Sensors Made from Carbon Nanotubes Based Polymer Nanocomposites. *Sensors* **2011,** *11* (11), 10691-10723.
29. Xu, H. P.; Dang, Z. M.; Jiang, M. J.; Yao, S. H.; Bai, J., Enhanced Dielectric Properties and Positive Temperature Coefficient Effect in the Binary Polymer Composites with Surface Modified Carbon Black. *J. Mater. Chem.* **2007,** *18* (2), 229-234.
30. Xu, H. P.; Dang, Z. M.; Bing, N. C.; Wu, Y. H.; Yang, D. D., Temperature Dependence of Electric and Dielectric Behaviors of Ni/Polyvinylidene Fluoride Composites. *J. Appl. Phys.* **2010,** *107* (3), 034105.
31. Kymakis, E.; Amaratunga, G. A., Electrical Properties of Single-Wall Carbon Nanotube-Polymer Composite Films. *J. Appl. Phys.* **2006,** *99* (8), 084302.

32. Peng, H., Aligned Carbon Nanotube/Polymer Composite Films with Robust Flexibility, High Transparency, and Excellent Conductivity. *J. Am. Chem. Soc.* **2008,** *130* (1), 42-43.
33. Choi, E. S.; Brooks, J. S.; Eaton, D. L.; Al-Haik, M. S.; Hussaini, M. Y.; Garmestani, H.; Li, D.; Dahmen, K., Enhancement of Thermal and Electrical Properties of Carbon Nanotube Polymer Composites by Magnetic Field Processing. *J. Appl. Phys.* **2003,** *94* (9), 6034-6039.
34. Bilotti, E.; Zhang, H.; Deng, H.; Zhang, R.; Fu, Q.; Peijs, T., Controlling the Dynamic Percolation of Carbon Nanotube Based Conductive Polymer Composites by Addition of Secondary Nanofillers: The Effect on Electrical Conductivity and Tuneable Sensing Behaviour. *Compos. Sci. Technol.* **2013,** *74*, 85-90.
35. Zhang, C.; Wang, P.; Ma, C.-a.; Wu, G.; Sumita, M., Temperature and Time Dependence of Conductive Network Formation: Dynamic Percolation and Percolation Time. *Polymer* **2006,** *47* (1), 466-473.
36. Electronic Industries Association Eia Rs-198c **1983**.
37. Yu, T.; Ni, Z.; Du, C.; You, Y.; Wang, Y.; Shen, Z., Raman Mapping Investigation of Graphene on Transparent Flexible Substrate: The Strain Effect. *J. Phys. Chem. C* **2008,** *112* (33), 12602-12605.
38. Xu, H. P.; Wu, Y. H.; Yang, D. D.; Wang, J. R.; Xie, H. Q., Study on Theories and Influence Factors of Ptc Property in Polymer-Based Conductive Composites. *Rev. Adv. Mater. Sci.* **2011,** *27* (2), 173-183.
39. Fang, L.; Shen, M. R.; Cao, W. W., Effects of Postanneal Conditions on the Dielectric Properties of Cacu3ti4o12 Thin Films Prepared on Pt/Ti/Sio2/Si Substrates. *J. Appl. Phys.* **2004,** *95* (11), 6483-6485.
40. Arlt, G.; Hennings, D., Dielectric Properties of Fine‐Grained Barium Titanate Ceramics. *J. Appl. Phys.* **1985,** *58* (4), 1619-1625.
41. Xie, S.-H.; Zhu, B.-K.; Wei, X.-Z.; Xu, Z.-K.; Xu, Y.-Y., Polyimide/Batio3 Composites with Controllable Dielectric Properties. *Compos. Part A: Appl. Sci. Manuf.* **2005,** *36* (8), 1152-1157.
42. Dang, Z. M.; Zhou, T.; Yao, S. H.; Yuan, J. K.; Zha, J. W.; Song, H. T.; Li, J. Y.; Chen, Q.; Yang, W. T.; Bai, J., Advanced Calcium Copper Titanate/Polyimide Functional Hybrid Films with High Dielectric Permittivity. *Adv. Mater. (Weinheim, Ger.)* **2009,** *21* (20), 2077-2082.
43. Qi, L.; Lee, B. I.; Chen, S.; Samuels, W. D.; Exarhos, G. J., High‐Dielectric‐Constant Silver−Epoxy Composites as Embedded Dielectrics. *Adv. Mater. (Weinheim, Ger.)* **2005,** *17* (14), 1777-1781.
44. Bai, J.; Zhong, X.; Jiang, S.; Huang, Y.; Duan, X., Graphene Nanomesh. *Nat. Nanotechnol.* **2010,** *5* (3), 190-194.
45. Yu, T.; Wang, F.; Xu, Y.; Ma, L.; Pi, X.; Yang, D., Graphene Coupled with Silicon Quantum Dots for High-Performance Bulk-Silicon-Based Schottky-Junction Photodetectors. *Adv. Mater. (Weinheim, Ger.)* **2016,** *28* (24), 4912-9.
46. Rao, C. N. R.; Gopalakrishnan, K.; Maitra, U., Comparative Study of Potential Applications of Graphene, Mos2, and Other Two-Dimensional Materials in Energy Devices, Sensors, and Related Areas. *ACS Appl. Mater. Interfaces* **2015,** *7* (15), 7809-7832.
47. Kuilla, T.; Bhadra, S.; Yao, D.; Kim, N. H.; Bose, S.; Lee, J. H., Recent Advances in Graphene Based Polymer Composites. *Prog. Polym. Sci.* **2010,** *35* (11), 1350-1375.
48. Xu, Z.; Gao, C., In Situ Polymerization Approach to Graphene-Reinforced Nylon-6 Composites. *Macromolecules* **2010,** *43* (16), 6716-6723.

49. Yan, L.; Zhao, B.; Liu, X.; Li, X.; Zeng, C.; Shi, H.; Xu, X.; Lin, T.; Dai, L.; Liu, Y., Aligned Nanofibers from Polypyrrole/Graphene as Electrodes for Regeneration of Optic Nerve Via Electrical Stimulation. *ACS Appl. Mater. Interfaces* **2016,** *8* (11), 6834-6840.
50. Yuan, J.; Luna, A.; Neri, W.; Zakri, C.; Schilling, T.; Colin, A.; Poulin, P., Graphene Liquid Crystal Retarded Percolation for New High-K Materials. *Nat. Commun.* **2015,** *6*, 8700.
51. Syurik, J.; Ageev, O.; Cherednichenko, D.; Konoplev, B.; Alexeev, A., Non-Linear Conductivity Dependence on Temperature in Graphene-Based Polymer Nanocomposite. *Carbon* **2013,** *63*, 317-323.
52. Pang, H.; Zhang, Y.-C.; Chen, T.; Zeng, B.-Q.; Li, Z.-M., Tunable Positive Temperature Coefficient of Resistivity in an Electrically Conducting Polymer/Graphene Composite. *Appl. Phys. Lett.* **2010,** *96* (25), 251907.
53. Wang, B.; Jiao, Y.; Gu, A.; Liang, G.; Yuan, L., Dielectric Properties and Mechanism of Composites by Superposing Expanded Graphite/Cyanate Ester Layer with Carbon Nanotube/Cyanate Ester Layer. *Compos. Sci. Technol.* **2014,** *91*, 8-15.
54. Wang, B.; Liang, G.; Jiao, Y.; Gu, A.; Liu, L.; Yuan, L.; Zhang, W., Two-Layer Materials of Polyethylene and a Carbon Nanotube/Cyanate Ester Composite with High Dielectric Constant and Extremely Low Dielectric Loss. *Carbon* **2013,** *54*, 224-233.
55. Wang, B.; Liu, L.; Huang, L.; Chi, L.; Liang, G.; Yuan, L.; Gu, A., Fabrication and Origin of High-K Carbon Nanotube/Epoxy Composites with Low Dielectric Loss through Layer-by-Layer Casting Technique. *Carbon* **2015,** *85*, 28-37.
56. Wang, B.; Liu, L.; Liang, G.; Yuan, L.; Gu, A., Boost up Dielectric Constant and Push Down Dielectric Loss of Carbon Nanotube/Cyanate Ester Composites Via Gradient and Layered Structure Design. *J. Mater. Chem. A* **2015,** *3* (46), 23162-23169.
57. Xu, H.-P.; Dang, Z.-M., Electrical Property and Microstructure Analysis of Poly (Vinylidene Fluoride)-Based Composites with Different Conducting Fillers. *Chem. Phys. Lett.* **2007,** *438* (4), 196-202.
58. Xiang, Z. D.; Chen, T.; Li, Z. M.; Bian, X. C., Negative Temperature Coefficient of Resistivity in Lightweight Conductive Carbon Nanotube/Polymer Composites. *Macromol. Mater. Eng.* **2009,** *294* (2), 91-95.
59. Ansari, S.; Giannelis, E. P., Functionalized Graphene Sheet—Poly (Vinylidene Fluoride) Conductive Nanocomposites. *J. Polym. Sci., Part B: Polym. Phys.* **2009,** *47* (9), 888-897.
60. Mathur, R. B.; Chatterjee, S.; Singh, B. P., Growth of Carbon Nanotubes on Carbon Fibre Substrates to Produce Hybrid/Phenolic Composites with Improved Mechanical Properties. *Compos. Sci. Technol.* **2008,** *68* (7–8), 1608-1615.

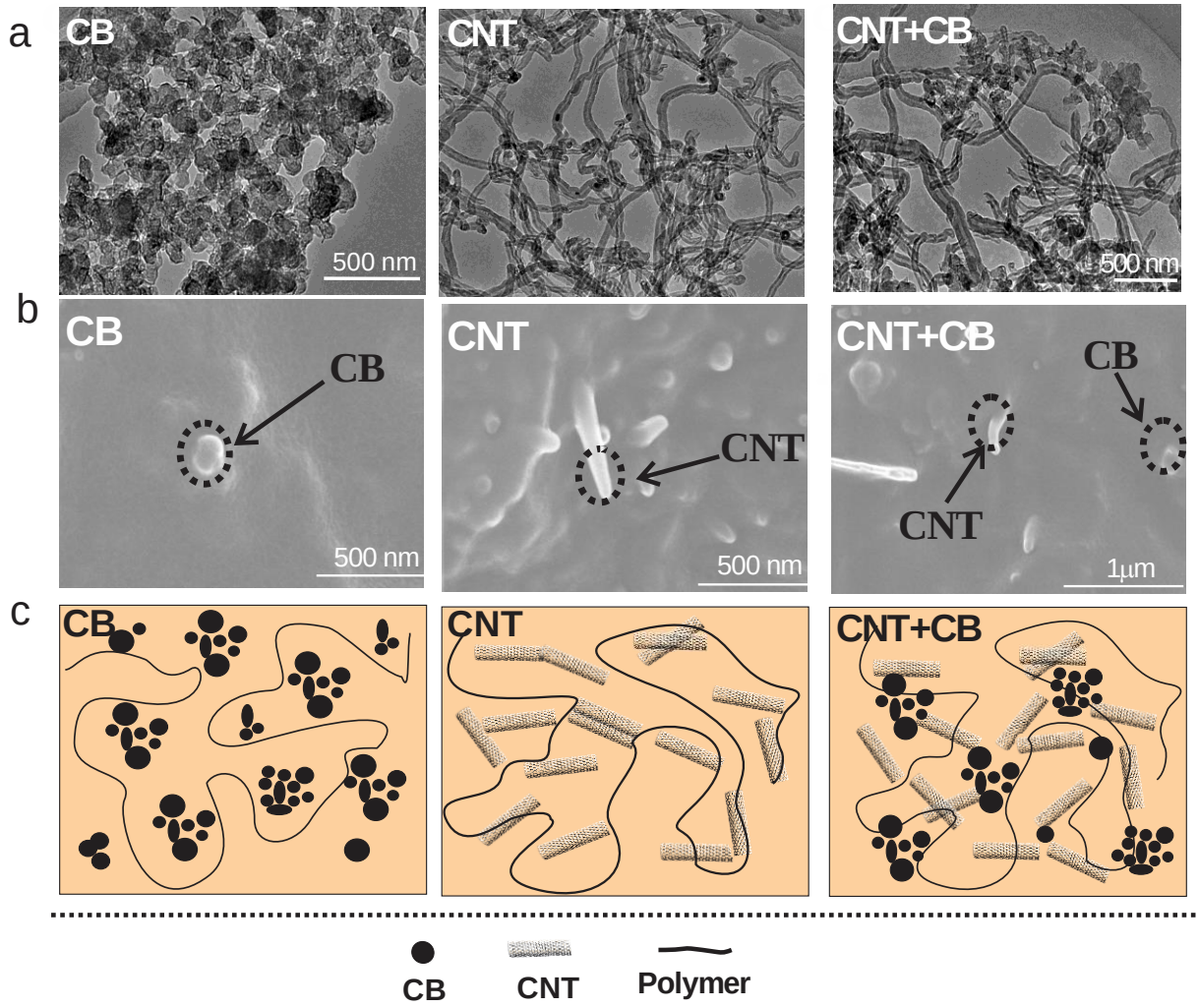
a
CB
500 nm
CNT
CNT+CB
500 nm
b
CB
CB
500 nm
CNT
CNT
500 nm
CNT+CB
CB
CNT
1μm
c
CB
CNT
CNT+CB
CB
CNT
Polymer

Figure – 1

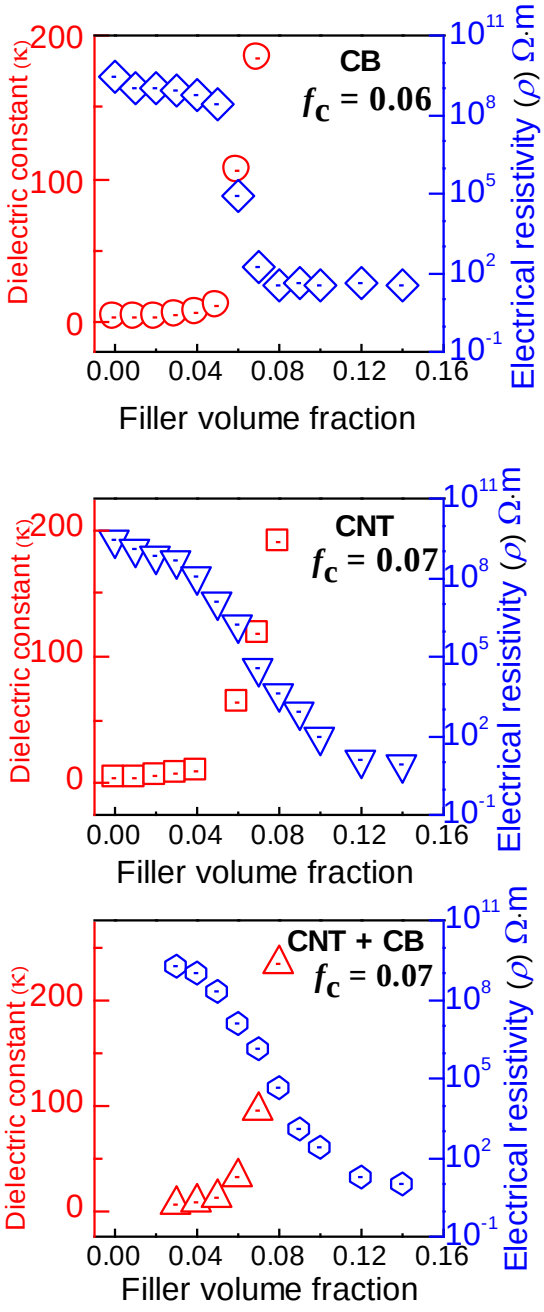
CB
f_c = 0.06
CNT
f_c = 0.07
CNT + CB
f_c = 0.07
Dielectric constant (κ)
Electrical resistivity (ρ) Ω·m
Filler volume fraction
0
100
200
0.00
0.04
0.08
0.12
0.16
10^{-1}
10^{2}
10^{5}
10^{8}
10^{11}

Figure – 2

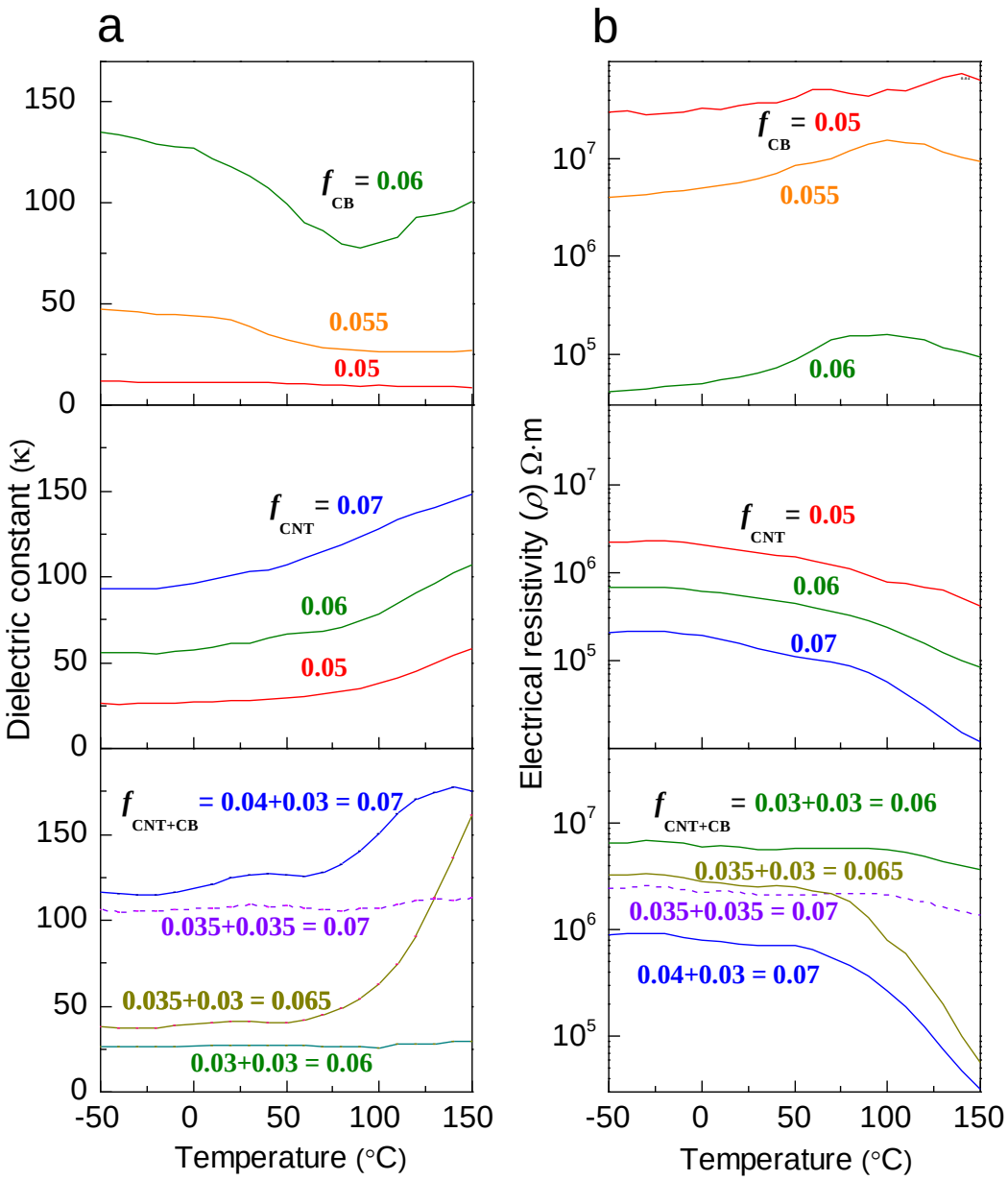
a
b
Dielectric constant (κ)
Electrical resistivity (ρ) Ω·m
Temperature (°C)
Temperature (°C)
f CB = 0.06
0.055
0.05
f CNT = 0.07
0.06
0.05
f CNT+CB = 0.04+0.03 = 0.07
0.035+0.035 = 0.07
0.035+0.03 = 0.065
0.03+0.03 = 0.06
f CB = 0.05
0.055
0.06
f CNT = 0.05
0.06
0.07
f CNT+CB = 0.03+0.03 = 0.06
0.035+0.03 = 0.065
0.035+0.035 = 0.07
0.04+0.03 = 0.07

Figure – 3

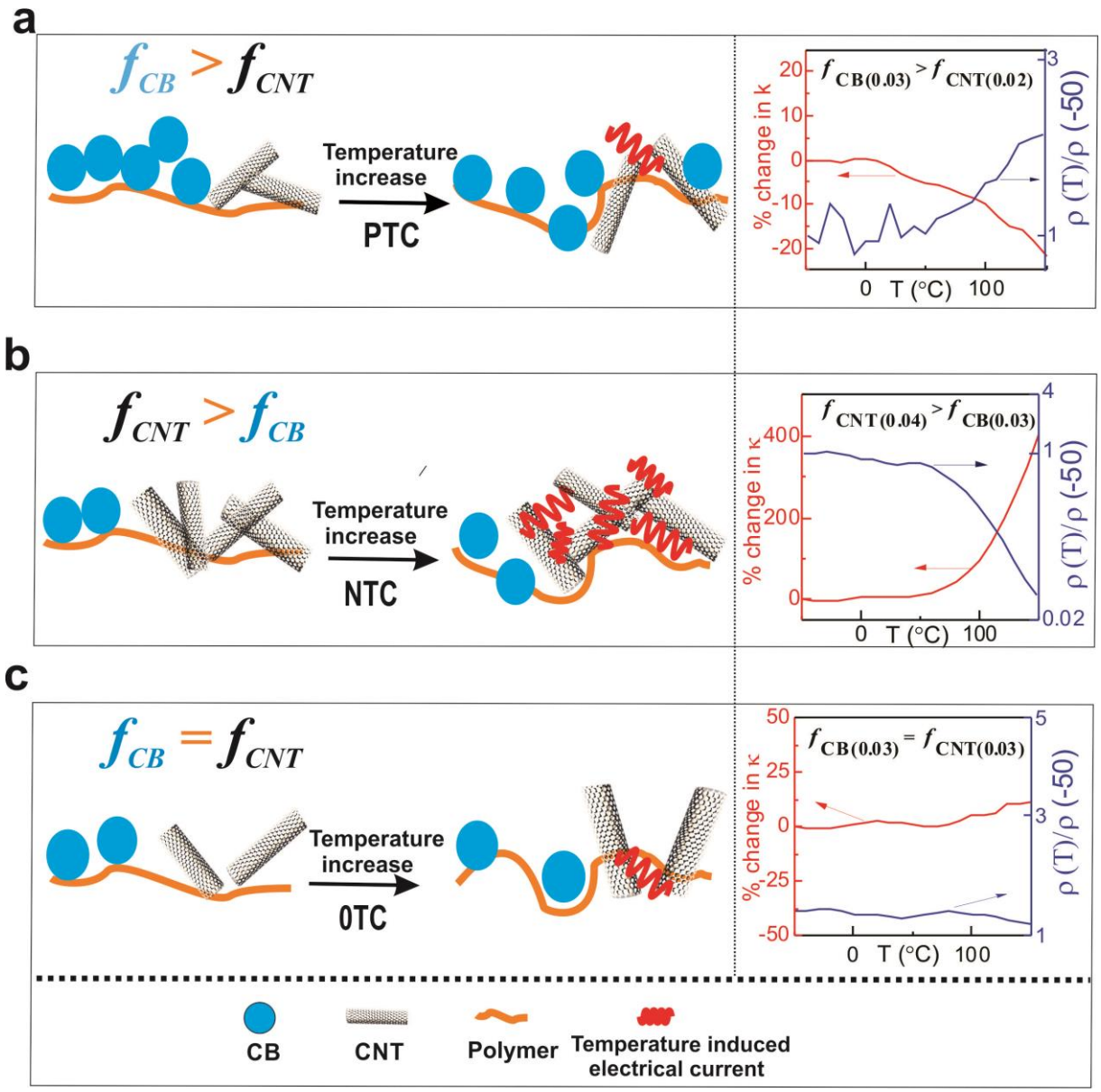
a
$f_{CB} > f_{CNT}$
Temperature increase
PTC
$f_{CB(0.03)} > f_{CNT(0.02)}$
% change in k
ρ (T)/ρ (-50)
0 T (°C) 100
b
$f_{CNT} > f_{CB}$
Temperature increase
NTC
$f_{CNT(0.04)} > f_{CB(0.03)}$
% change in κ
ρ (T)/ρ (-50)
0 T (°C) 100
c
$f_{CB} = f_{CNT}$
Temperature increase
0TC
$f_{CB(0.03)} = f_{CNT(0.03)}$
% change in κ
ρ (T)/ρ (-50)
0 T (°C) 100
CB
CNT
Polymer
Temperature induced electrical current

Figure – 4

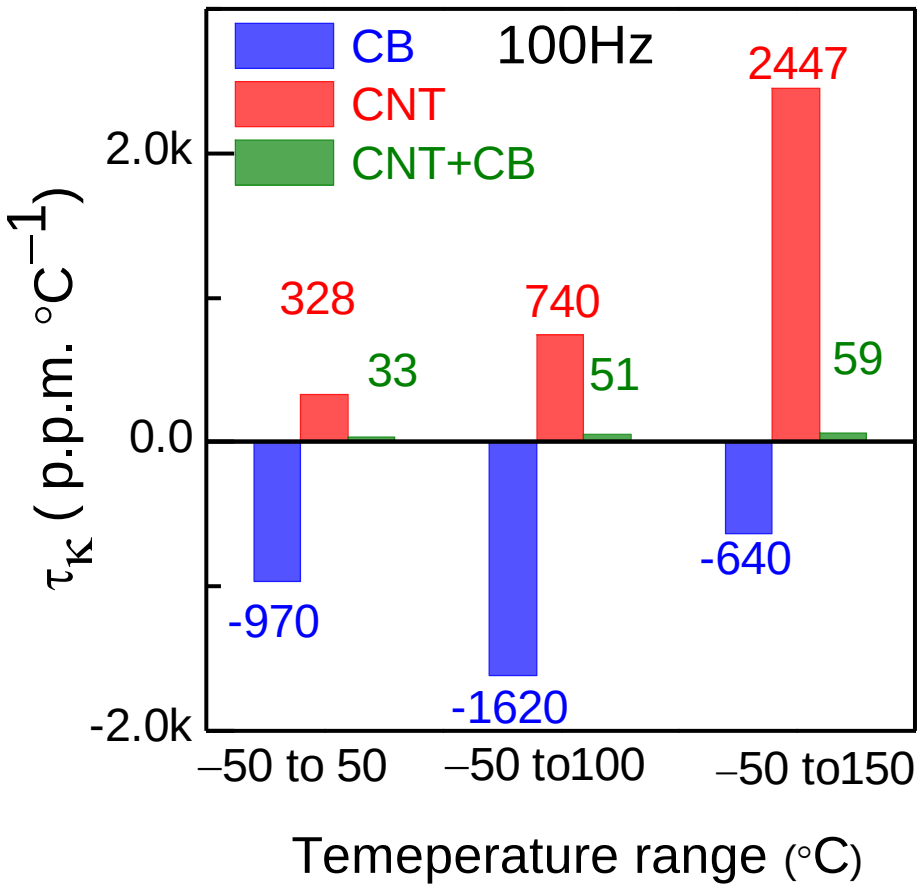
CB
CNT
CNT+CB
100Hz
2.0k
0.0
-2.0k
τ_K (p.p.m. °C^{-1})
328
33
740
51
2447
59
-970
-1620
-640
–50 to 50
–50 to100
–50 to150
Temeperature range (°C)

Figure – 5

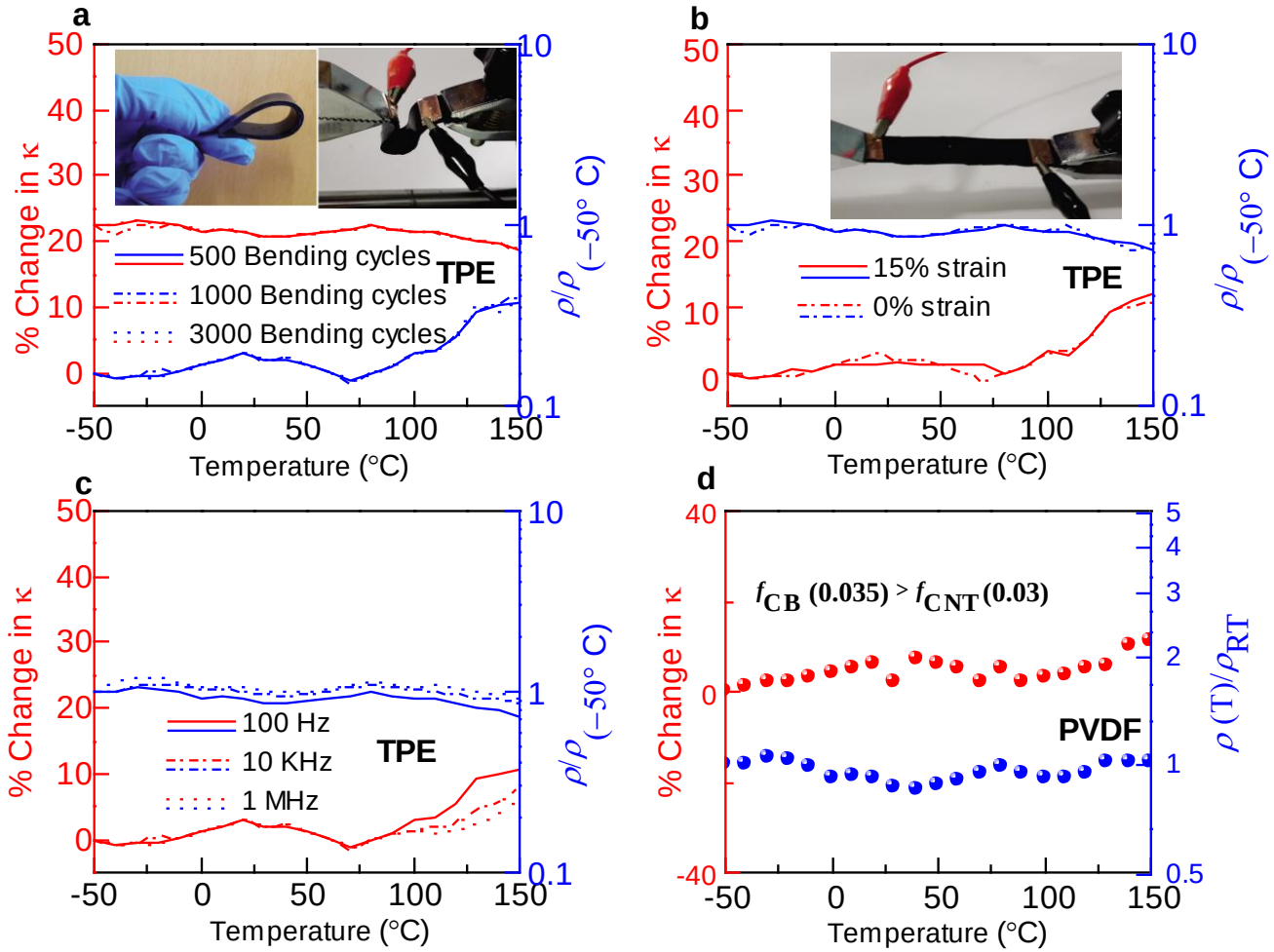
a
% Change in κ
ρ/ρ(−50° C)
500 Bending cycles
1000 Bending cycles
3000 Bending cycles
TPE
Temperature (°C)
b
15% strain
0% strain
TPE
c
100 Hz
10 KHz
1 MHz
TPE
d
f_{CB} (0.035) > f_{CNT} (0.03)
PVDF
ρ (T)/ρRT

Figure – 6

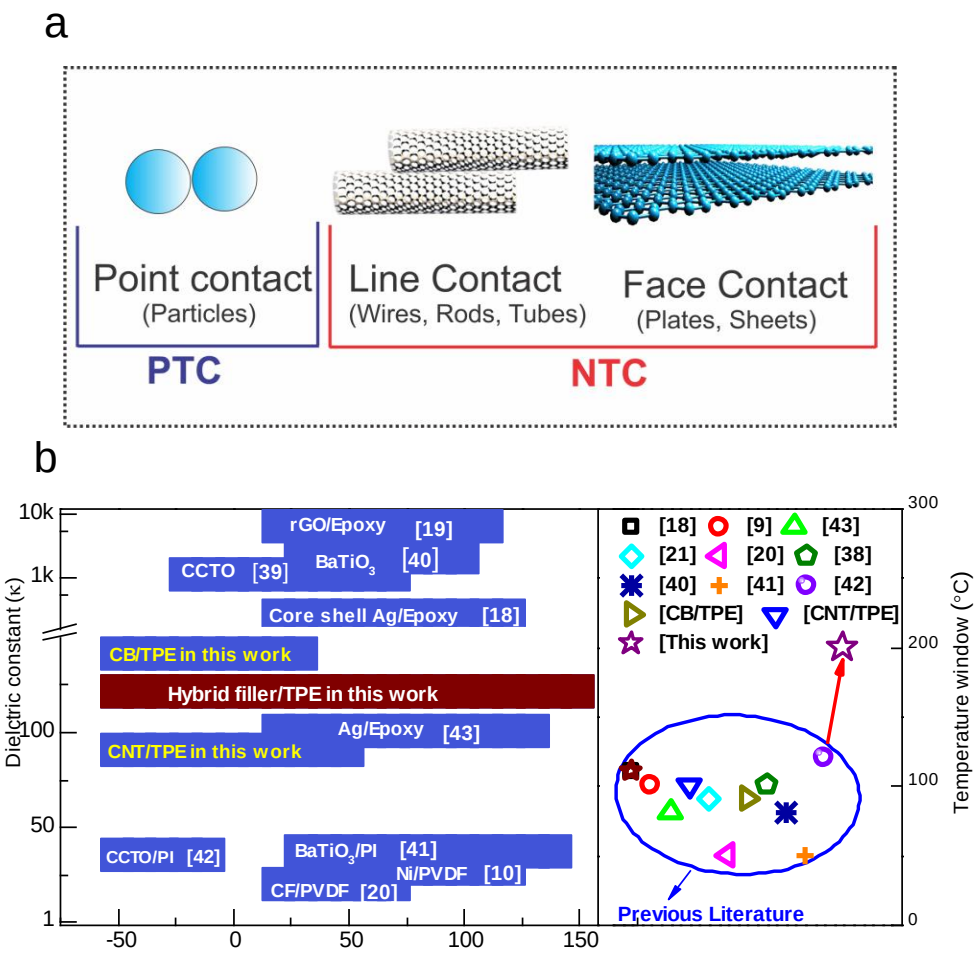
a
Point contact
(Particles)
Line Contact
(Wires, Rods, Tubes)
Face Contact
(Plates, Sheets)
PTC
NTC
b
Dielectric constant (κ)
10k
1k
100
50
1
-50
0
50
100
150
rGO/Epoxy [19]
CCTO [39]
BaTiO3 [40]
Core shell Ag/Epoxy [18]
CB/TPE in this work
Hybrid filler/TPE in this work
Ag/Epoxy [43]
CNT/TPE in this work
CCTO/PI [42]
BaTiO3/PI [41]
Ni/PVDF [10]
CF/PVDF [20]
[18] [9] [43]
[21] [20] [38]
[40] [41] [42]
[CB/TPE] [CNT/TPE]
[This work]
Previous Literature
300
200
100
0
Temperature window (°C)

Figure – 7

Figure captions

Fig. 1. (a) TEM images of carbon fillers. **(b)** SEM micrographs of all three carbon filler/polymer composites. **(c)** Schematics of carbon filler networks in polymer matrix.

Fig. 2. Percolation curves of dielectric constant @100Hz and electrical resistivity of composites at various filler concentrations,

Fig. 3. (a) Electrical resistivity of composites as a function of temperature at various filler concentrations below, at, and above percolation threshold). **(b)** Dielectric constant @100Hz of composites as a function of temperature at various filler concentrations near the percolation threshold.

Fig. 4. Schematics and electrical resistivity/dielectric constant plots of CNT+CB hybrid filler composites with **(a)** PTC, **(b)** NTC, and **(c)** L/0TC characteristics.

Fig. 5. Temperature coefficient of dielectric constant of composites in different temperature ranges.

Fig. 6. L/0TC characteristics of electrical and dielectric properties of CNT+CB hybrid filler/TPE polymer composites **(a)** after various bending cycles, **(b)** stretching along the length, **(c)** at different AC frequencies. **(d)** L/0TC electric characteristics of CNT+CB hybrid filler/PVDF polymer composites.

Fig. 7. (a) Summary of different inter-filler contact types and most probable temperature coefficient of electrical resistivity associated with their corresponding polymer composites. **(b)** Comparison of our results with previous studies.